Response of superfluid vortex filaments to concentrated normal-fluid vorticity

David C. Samuels
Center for Turbulence Research, Stanford University, Stanford, California 94305
(Received 3 August 1992)

We simulate the motion of quantized vortex filaments moving under the influence of concentrated vorticity in the normal fluid. These simulations show an exponential growth of ordered superfluid vortex filaments in the core of the normal-fluid vortex. We explain the cause of this growth and develop formulas for the growth time scales and the minimum normal-fluid vortex circulation that causes this growth. Finally, we compare these values to the lifetime and circulation of the vortex tubes, which should be present in the classical turbulence of the normal fluid.

Helium II behaves as a superposition of two fluids: a normal fluid and a superfluid. The superfluid component contains vortex filament with an atomic scale core radius, $a_0 \approx 1$ Å, and a quantized circulation κ. The normal-fluid component is a classical fluid with a small viscosity μ_n. Each fluid has its own density ρ_n and ρ_s and velocity field $\mathbf{v}_n$ and $\mathbf{v}_s$, where the subscripts refer to the normal fluid and superfluid, respectively. The two fluids interact through mutual friction caused by the scattering of the normal fluid by the superfluid vortex filaments.

Experiments and simulations[1] with the normal fluid and superfluid flowing in opposite directions (loosely defined as "counterflow") show that the superfluid vortex filaments form a self-sustaining tangle of individual filaments, with a dissipation due to the relative velocity between the fluids. This behavior is very unlike classical turbulence. In contrast, recent experiments[2,3] with superfluid and normal-fluid flows in the same direction ("coflow") have given results which are most easily interpreted as the flow of a single fluid of density $\rho=\rho_n+\rho_s$ and viscosity μ_n. Particularly convincing are the experiments by Borner and Schmidt[3] which measured separately the circulations of the normal fluid and the superfluid in a large vortex ring produced by a piston. They found that the normal-fluid and superfluid circulations were equal in magnitude and spatial distribution through the vortex ring at all times measured. It has been suggested by Donnelly[4] that in coflow the superfluid vortex filaments are driven to mimic the circulation field of the normal fluid, yielding a state which is hydrodynamically similar to a Navier-Strokes fluid. This state may be a useful tool for the study of Navier-Stokes turbulence. It definitely has important consequences for cryogenic engineering. Previously, we have had no theoretical understanding of this state. In this work we describe a basic process which drives the superfluid circulation to locally match the normal-fluid circulation in turbulent flows.

The superfluid vortex filaments move as vortex filaments in an ideal fluid with the addition of motion due to the mutual friction with the normal fluid. This equation of motion is

$$d\mathbf{s}/dt=\mathbf{v}_s+\mathbf{v}_I+\alpha\mathbf{s}'\times(\mathbf{v}_n-\mathbf{v}_s-\mathbf{v}_I)\ , \tag{1}$$

where $\mathbf{s}$ is the position of a point on the vortex filament, $\mathbf{v}_I$ is the self-induced velocity of the vortex filament, α is a temperature-dependent coefficient of mutual friction, and a prime denotes a derivative by arclength. We solve this equation by a Runge-Kutta-Fehlberg method. The self-induced velocity is given by the Biot-Savart law

$$\mathbf{v}_I(\mathbf{s})=\frac{\kappa}{4\pi}\int\frac{(\boldsymbol{\xi}-\mathbf{s})\times d\boldsymbol{\xi}}{|\boldsymbol{\xi}-\mathbf{s}|^3}\ , \tag{2}$$

where the integral is taken over all filaments in the fluid. The singularity inherent in the Biot-Savart law is handled by a method due to Schwarz.[5] In some situations a local approximation of Eq. (2) is useful. The local induction approximation (LIA) is $\mathbf{v}_I=\beta s'\times s''$, where $\beta=(\kappa/4\pi)\ln(AR/a_0)$, R is the local radius of curvature of the filament, and A is a constant of order 1. We use the Biot-Savart law except where expressly indicated.

Through mutual friction, the superfluid vortex filament is influenced by the normal-fluid velocity field $\mathbf{v}_n$. In the present simulations $\mathbf{v}_n$ is held constant but nonuniform. We are interested in the behavior of superfluid vortex filaments in turbulent $\mathbf{v}_n$ fields. As a simple model of this, we use a single normal-fluid vortex tube to represent the fine scale structure[6-12] of the turbulent normal fluid. Specifically, we use a Gaussian distribution of vorticity about the Z axis. The resulting velocity field is

$$\mathbf{v}_n(r)=\frac{\Gamma_n\kappa}{2\pi r}[1-\exp(-r^2/r_c^2)]\hat{\boldsymbol{\phi}}\ , \tag{3}$$

where Γ_n is the total normal-fluid circulation in units of κ, r is the radius from the Z axis, and we shall call r_c the core radius. We define the normal-fluid circulation inside the core radius as $\Gamma_{nc}\simeq 0.63\Gamma$. In order to have a finite-size simulation, the normal-fluid vortex is cut off arbitrarily at $Z=\pm L$ by rapidly increasing the core radius [see Fig. 1(a)]. This is artificial, but it serves our purpose of forming a simple model of the vortex tubes. We have found little dependence of any behavior on L. For the results presented in this work we have used $L=10r_c$.

We initiate the simulations with a small superfluid vortex ring located a few core diameters r_c from the normal-fluid vortex core with its velocity vector pointed approximately towards the vortex tube [Fig. 1(a)]. The ring

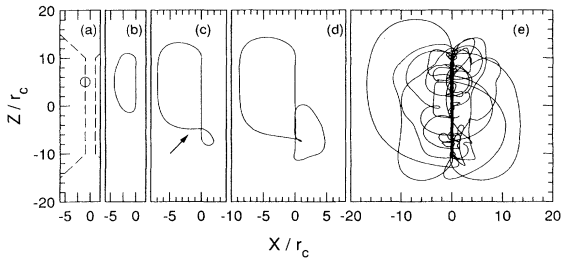

FIG. 1. Evolution of the superfluid vortex filament. The simulation parameters are $\Gamma_{nc}=76$, $\alpha=0.25$, and $r_c=10^{-3}$ cm. (a) $t=0.0$. The solid lines denote superfluid vortex filaments. The dashed lines outline the normal-fluid vortex core. (b) $t=0.003$ sec. (c) $t=0.0066$ sec. The arrow marks the site of the Glaberson instability. (d) $t=0.01$ sec. A new loop forms. (e) $t=0.03$ sec. Superfluid vortex filaments are concentrated in the core of the normal-fluid vortex.

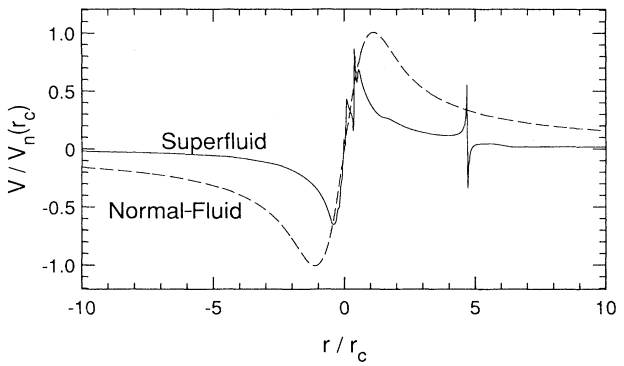

FIG. 2. Superfluid and normal-fluid velocity profiles at $t=0.0363$ sec. Velocities are normalized by the maximum v_n.

moves toward the vortex tube by its own self-induced velocity until one side of the ring is captured by the normal-fluid vortex core through mutual friction. The side of the ring which is captured is always the side with the circulation vector in the same direction as the normal-fluid circulation vector. After capture, the ring is stretched along the axis of the vortex tube, again by mutual friction [Fig. 1(b)]. As the ring is stretched, it will also rotate about the axis of th vortex tube due to its self-induced velocity. The ends of the elongated vortex loop rotate the fastest since their curvature is greatest [Fig. 1(b)]. This differential rotation of the loop twists sections of the superfluid vortex filament and leads to a normal-fluid velocity along the filament in these sections. An axial normal-fluid flow along a superfluid filament was shown by Ostermeier and Glaberson[13] to cause an instability of the filament to the growth of helical waves. In Fig. 1(c), the arrow indicates a section of the superfluid vortex filament where the Glaberson instability is beginning to grow. From this instability a new loop of vortex filament forms (we occasionally observed multiple loops forming simultaneously at single instability site, but a single loop is typical). This new loop is also captured by the normal-fluid vortex tube [Fig. 1(d)] and it repeats the behavior of the initial loop. The original instability site continues to produce new loops until it grows beyond the end of the normal-fluid vortex tube. This process of loop generation leads to an exponential growth of the length of superfluid vortex filament. After a few repetitions of this, a dense concentration of ordered superfluid vortex filaments forms inside the core of the normal-fluid vortex tube [Fig. 1(e)]. The density of these filaments is equal to the local vorticity density of the normal fluid (see Fig. 2).

The essential step in this process of exponential growth is the formation of new vortex loops by the Glaberson instability. With this in mind, it is easy to see that the initial conditions are unimportant to the growth. The true beginning of this growth is in Fig. 1(c) on the section of filament marked by the arrow, not in Fig. 1(a). This growth could just as well be started from a low curvature superfluid vortex filament which happens to come near the normal-fluid vortex tube. The initial conditions of these simulations were chosen solely for computational convenience.

In Fig. 2, we show the azimuthal velocity of both the normal fluid and the superfluid taken along an arbitrary test line (the X axis) through the vortex tube at $Z=0$. The two velocity fields are well matched in a significant region of the normal-fluid vortex core, and the superfluid velocity outside the vortex core is increasing toward the normal-fluid velocity. The sharp spikes in superfluid show very close approaches of individual vortex filaments to the test line. The simulation was stopped at this point because the CPU time per simulation time step had grown impractically large due to the time necessary to calculate the Biot-Savart law for a large length of vortex filament. In Fig. 3, we show the circulations of both the normal fluid and the superfluid inside the core radius. The growth is exponential. By the end of the simulation the superfluid circulation had grown to 36% of the normal-fluid circulation and was still growing smoothly with no indication that this growth was stopping. Since the Glaberson instability is driven by the relative velocity $\mathbf{v}_{ns}=\mathbf{v}_n-\mathbf{v}_s$ we expect that this growth will cease when $\mathbf{v}_{ns}$ is zero (and therefore $\Gamma_s=\Gamma_n$). It is possible that the growth of the superfluid circulation will actually cease at some earlier point. At the present time we can make no determination of when the growth stops.

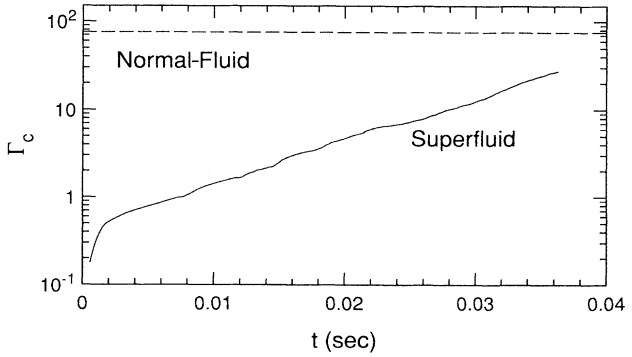

FIG. 3. Exponential growth of the superfluid circulation inside the normal-fluid vortex core. The dashed line denotes the normal-fluid circulation.

We calculated the time scale of this exponential growth as a function of α and r_c. In these simulations we used the LIA. This was necessary in order to do a large number of simulations over a time long enough to compute the growth time scale in each simulation. From these simulations we developed an equation for the growth time τ,

$$\tau=\frac{Cr_c^2}{\sqrt{\alpha}\kappa\Gamma_{nc}}\ , \tag{4}$$

where τ is defined from the equation $\Gamma_{sc}(t)=\Gamma_{sc}(0)\exp(t/\tau)$. The constant C was determined by a least-squares fit to be $C=458\pm5$. We plot τ from the simulations against the values from Eq. (4) in Fig. 4. Each data set plotted extends over a range of $75<\Gamma_{nc}<200$. The fit is quite good except for simulations with both low Γ_{nc} and $\alpha\leq0.2$, in which case the observed growth time scales are shorter than the predicted values.

Below a minimum Γ_{nc} the Glaberson instability is not seen in the simulations. We plot this minimum circulation as a function of α and r_c in Fig. 5. These data were taken with LIA simulations. From least-squares fits of this data we have the formula

$$\Gamma_{nc,\min}=\frac{D}{\alpha}\ln\left[\frac{8r_c}{a_0}\right]-E\ , \tag{5}$$

where $D=1.30\pm0.05$ and $E=7.8\pm0.3$. This equation gives the solid lines in Fig. 5. We have no explanation for the low α behavior. From direct numerical simulations (DNS) of Navier-Stokes turbulence Jimenez[14] has calculated the circulation of the vortex tubes. He defines a circulation Reynolds number $\mathrm{Re}_\gamma=\gamma/\nu$ where γ is the circulation of the vortex tube and ν is the kinematic viscosity of the fluid. He finds that the vortex tubes in the simulations fall in the range $200<\mathrm{Re}_\gamma<400$. It is not yet known if this range is constant or dependent on the flow Reynolds number. With this caveat, we will consider the range of Re_γ to be constant. With this we calculate the expected vortex tube circulation in the normal fluid

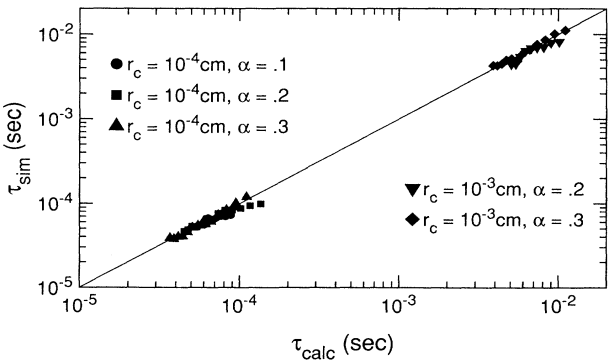

FIG. 4. Time scales of the exponential growth of the superfluid circulation. Values taken from simulations are compared to Eq. (4).

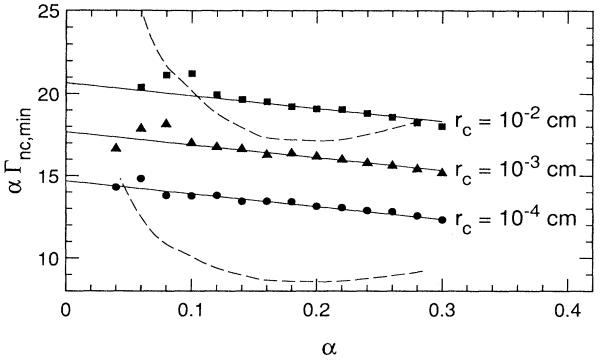

FIG. 5. Minimum Γ_{nc} for the Glaberson instability vs α. The solid lines are from Eq. (5). The dashed lines outline the expected range of circulations for the normal-fluid vortex tubes [Eq. (6)].

$$\Gamma=\mathrm{Re}_\gamma\left[\frac{\rho}{\rho_n}\right]\left[\frac{\nu}{\kappa}\right]\ , \tag{6}$$

where $\nu=\mu_n/\rho$. The range of Eq. (6) for $200<\mathrm{Re}_\gamma<400$ is outlined in Fig. 5 by the dashed lines. Comparing the simulation data with this expected range of vortex tube circulations, we see that core sizes on the order of 10^{-3} cm or less are needed for this instability. From DNS (Refs. 9, 11, and 14) the core radius of the vortex tubes is found to be $r_c\simeq3\eta$, where η is the Kolmogorov length. Again, this value is taken from low Reynolds number DNS and could be dependent on Reynolds number. The reader should remember that the simulation results shown in Fig. 5 are for straight and uniform normal-fluid vortex tubes. Curves or local nonuniformities in the tubes may decrease the minimum Γ_n by locally increasing the normal-fluid velocity along the superfluid vortex filament.

In experiments using water, Doudy, Carder, and Brachet[12] state that the lifetime of these vortex tubes is approximately one large eddy turnover time. In terms of the Reynolds number $\mathrm{Re}=\rho_n U_I L_I/\mu_n$, where U_I and L_I are the velocity and length scales of the large eddies, this time is $t_I=\pi L_I^2\rho_n/\mathrm{Re}\nu\rho$. If we take the ratio of t_I to τ and use Eq. (6) and the relation $\eta\simeq L_I\mathrm{Re}^{-3/4}$ from Navier-Stokes turbulence,[15] we have

$$t_I/\tau\simeq(0.23\pm0.08)\sqrt{\alpha}\mathrm{Re}^{1/2}\ . \tag{7}$$

So, for Reynolds numbers on the order of 1000 or higher we expect the vortex tube lifetime to be large compared to the growth time scale τ.

Our analysis has been conducted under the assumption that the normal-fluid vortex tube is stationary in the rest frame of the average superfluid velocity. This is a good approximation for the coflowing state, but is not true for the counterflow state. The superfluid vortex filaments shown in Fig. 1 are held and aligned through mutual friction by a region inside the normal-fluid vortex core where the relative velocity $\mathbf{v}_{ns}$ initially was zero.[16] In these simulations, this region was the Z axis where $\mathbf{v}_n=\mathbf{v}_s=0$. Without this region, the superfluid vortex filaments will

not be captured by the normal-fluid vortex. It is unlikely that such a region will exist in a counterflow state, so we expect that the process described in this work only occurs in a coflowing state. In summary, we have identified a process, specific to the coflowing state, which causes the exponential growth of concentrated and ordered superfluid vortex filaments inside the cores of the normal-fluid vortex tubes present in turbulent flows.

[1]K. W. Schwarz, Phys. Rev. B **38**, 2398 (1988).
[2]P. L. Walstrom, J. G. Weisend, II, J. R. Maddocks, and S. W. Van Sciver, Cyrogenics **28**, 101 (1988).
[3]H. Borner and D. W. Schmidt, in *Flow of Real Fluids,* Lecture Notes in Physics Vol. 235, edited by G. E. A. Meier and F. Obermeier (Springer, Berlin, 1985), p. 135.
[4]R. J. Donnelly, in *High Reynolds Number Flows Using Liquid and Gaseous Helium,* edited by R. J. Donnelly (Springer-Verlag, New York, 1991), p. 3.
[5]K. W. Schwarz, Phys. Rev. B **31**, 5782 (1985).
[6]A. Y. Kuo and S. Corrsin, J. Fluid Mech. **56**, 447 (1972).
[7]E. C. Siggia, J. Fluid Mech. **107**, 375 (1981).
[8]R. M. Kerr, J. Fluid Mech. **153**, 31 (1985).
[9]A. Vincent and M. Meneguzzi, J. Fluid Mech. **225**, 1 (1991).
[10]Z. S. She, E. Jackson, and S. A. Orszag, Nature (London) **344**, 226 (1990).
[11]G. R. Ruetsch and M. R. Maxey, Phys. Fluid A **3**, 1587 (1991).
[12]S. Doudy, Y. Couder, and M. E. Brachet, Phys. Rev. Lett. **67**, 983 (1991).
[13]R. M. Ostermeier and W. I. Glaberson, J. Low Temp. Phys. **21**, 191 (1975).
[14]J. Jimenez, Phys. Fluids A **4**, 652 (1992).
[15]A. S. Monin and A. M. Yaglom, *Statistical Fluid Mechanics II* (MIT Press, Cambridge, 1975), pp. 198–200.
[16]D. C. Samuels, Phys. Rev. B **46**, 11 714 (1992).